Available online at www.eccomasproceedia.org
Eccomas Proceedia COMPDYN (2025) 5248-5256

ECCOMAS
Proceedia

COMPDYN 2025
10th ECCOMAS Thematic Conference on
Computational Methods in Structural Dynamics and Earthquake Engineering
M. Papadrakakis, M. Fragiadakis (eds.)
Rhodes Island, Greece, 15-18 June 2025

CYCLIC BEHAVIOR OF STAINLESS STEEL BEAM-COLUMN JOINTS: NONLINEAR FE PARAMETRIC STUDY

Shafayat Bin Ali[1], **George S. Kamaris**[2], **Edmond Muho**[3], **and George Papagiannopoulos**[2]

[1] Department of Disaster Engineering and Management, Chittagong University of Engineering &Technology
Chattogram-4349, Bangladesh
e-mail: shafayat@cuet.ac.bd

[2] School of Science and Technology, Hellenic Open University
Patras GR-26335, Greece
e-mail: gekamaris@gmail.com, {georgios.kamaris,papagiannopoulos}@eap.gr

[3] College of Civil Engineering, Tongji University
Shanghai, China
e-mail: edmondmuho@tongji.edu.cn

Abstract

Stainless steel structural members offer notable ductility and strain hardening capacity, making them particularly promising for seismic applications. However, the lack of simplified modeling approaches often necessitates advanced nonlinear three-dimensional finite element (FE) simulations to accurately capture their cyclic response. In this study, a nonlinear FE model is developed and validated against experimental results, accurately reproducing both local and global buckling, mainly observed in the lower region of the beam. Following FE validation, fifteen beam-column assemblies with different IPE sections are analyzed under cyclic loading according to American Institute of Steel Construction *(AISC) protocols, enabling a comprehensive parametric investigation of the effects of beam cross section size. The results show clear hysteresis loops and stable energy dissipation for all specimens, with larger beam sections exhibiting enhanced stiffness, strength and flexural capacity. Finally, backbone curves derived from the FE analyses provide essential parameters, including yield strength, ultimate strength and maximum bending moment, for a varied range of beam geometries. These backbone curves offer valuable data for practical seismic design and performance assessment of stainless steel beam-column joints, thus reducing reliance on extensive FE simulations in practical analysis and design applications.*

Keywords: Stainless steel; Beam-column joints; Nonlinear finite element analysis; Cyclic behavior; Hysteresis; Backbone curves; Parametric investigation; Seismic performance; IPE sections

ISSN:2623-3347
Peer-review under responsibility of the organizing committee of COMPDYN 2025.
doi: 10.7712/120125.12808.25885

1 INTRODUCTION

Stainless steel has gained increasing acceptance in construction due to its exceptional durability, corrosion resistance and aesthetic appeal. In addition to these advantages, its high strength and ductility make it particularly suitable for seismic design. Its ability to sustain large inelastic deformations while dissipating energy efficiently supports the objectives of performance-based earthquake engineering (PBEE) and seismic-resilient design, which seek to ensure that structures meet defined performance targets under varying seismic demands [1,2].

Within PBEE frameworks, reliable models of component hysteresis and backbone curves are essential for predicting engineering demand parameters, such as displacement, moment capacity and energy dissipation [3,4]. Despite the promising characteristics of stainless steel, the limited availability of cyclic response data for stainless steel beam-column joints has hindered the development of robust predictive models and comprehensive component databases, thereby limiting the ability to accurately assess seismic risks in such structures.

Addressing this gap, the present study employs a nonlinear finite element (FE) analysis using a high-fidelity FE model to simulate the cyclic behavior of welded stainless steel beam-column joints under loading protocols prescribed by the American Institute of Steel Construction (AISC). The model is calibrated to accurately replicate experimental responses and a parametric investigation is conducted on fifteen FE models that incorporate different IPE beam sections. The objective is to evaluate how variations in beam geometry influence seismic performance metrics, with particular focus on stiffness, strength and energy dissipation. Additionally, backbone curves are derived to capture both elastic and inelastic behavior. Backbone curves extracted from the FE analysis provide key parameters, including yield strength, ultimate strength and maximum bending moment, that can reduce reliance on extensive FE simulations in practical analysis and design applications.

This paper is organized as follows. Section 2 describes the finite element modelling and calibration. Section 3 presents the experimental study used for model validation. Section 4 details the simulation setup. Section 5 discusses the parametric results, including failure modes, hysteresis behavior and backbone curves. Section 6 concludes with key findings and their implications for seismic design.

2 PARAMETRIC STUDY

To examine the cyclic response of stainless steel beams, a parametric study was conducted using different IPE sections. A total of 15 IPE sections were used, the characteristics of which are shown in Table 1 and Fig. 1. All the sections used herein are Class 1 and 2 because these are the only classes allowed by EC8 [5] for the seismic design of steel structures.

3 EXPERIMENTAL STUDY

The finite element model that is used for the parametric study of this work was validated based on the experimental results of Wei et al. [6]. A total of 6 specimens were designed and tested in [6], applying the AISC cyclic loading protocol [7]. The specimens were scaled joints which were extracted from the exterior moment-resisting frame (MRF) shown in Figure 1 of the prototype building of Figure 1 (a)[8]. The test set-up of this experimental study is depicted in Figure 1(b).

No	Section ID	Dimensions (H×B×t_w×t_f) (mm)
1	IPE80	80×46×3.8×5.2
2	IPE100	100×55×4.1×5.7
3	IPE120	120×64×4.4×6.3
4	IPE140	140×73×4.7×6.9
5	IPE160	160×82×5×7.4
6	IPE180	180×91×5.3×8
7	IPE200	200×100×5.6×8.5
8	IPE220	220×110×5.9×9.2
9	IPE240	240×120×6.2×9.8
10	IPE270	270×135×6.6×10.2
11	IPE300	300×150×7.1×10.7
12	IPE330	330×160×7.5×11.5
13	IPE360	360×170×8.0×12.7
14	IPE400	400×180×8.6×13.5
15	IPE450	450×190×9.4×14.6

Table 1: IPE sections used in the parametric study.

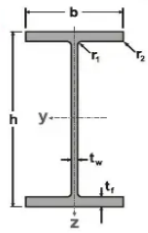

Figure 1: Typical IPE section.

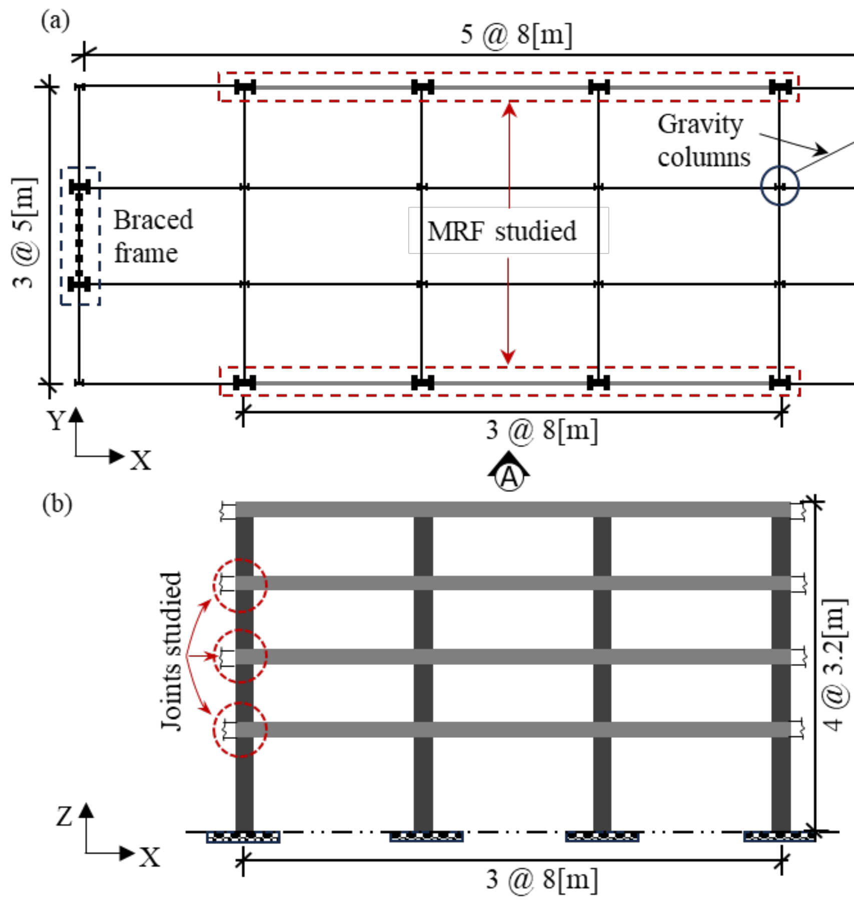

Figure 1: Prototype building: (a) Plan view; and (b) Elevation A.

4 FINITE ELEMENT MODELLING

To study the hysteresis behavior of stainless-steel beam-column joint a nonlinear FE model was developed using ABAQUS [9] software. The developed FE model was validated in terms of experimental data to accurately predict the hysteresis behavior and failure modes of the joint [6]. This study used this validated FE model to generate fifteen FE specimens where varying IPE sections were considered for the beam. In this FE model, the beam and column were modelled using four-node shell elements with reduced integration (S4R) which has been successfully applied in past research studies to simulate the cyclic behavior of steel section joints [10-12]. Tie constraints were used for all welded connections of the beam-column joint specimens. Based on the mesh sensitivity study, a 10 × 10 mm mesh size was selected to discretize all FE specimens. The average nonlinear material response of tensile coupon tests presented by Wei et al. [6] was considered to simulate the mechanical behavior of all IPE sections. The von Mises yield criterion is used to define the yielding of the stainless steel. To replicate the hysteresis response of the beam-column joint the Chaboche approach was applied, where the yield stress, plastic strain and maximum variation of yield surface were taken as 150 MPa, 10 and 5000 MPa based on test data [6], respectively. Boundary conditions of test setup were properly adopted in the FE models. Translational and rotational degrees of freedom of the bottom flange of the horizontal member were fixed as the movement and rotation of the horizontal member were restrained during the test. As out-of-plane deformation of the vertical member was prevented using bracing during the test, hence at the bracing point horizontal displacement in the x-direction of the vertical member was restrained. The cyclic force was employed on the vertical member using a reference point which was tied to the outer face of the member. The static general solver was adopted to solve this nonlinear analysis. In the FE models, residual stresses generated due to welding are considered in the beam only as no significant deformation was not noticed in the column. Values of the residual stress are calculated according to the pattern given by Yuan et al. [13]. Figure 2 shows the details of FE modelling, including geometry, boundary condition and loading point.

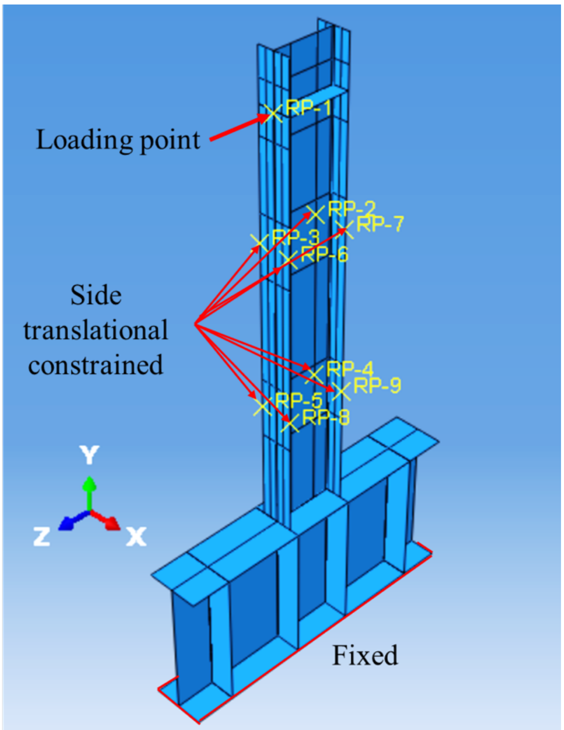

Fig. 2: Geometry, boundary condition and loading point of a typical FE model.

5 RESULTS AND DISCUSSION

The failure patterns of all specimens were investigated after the analysis. It is observed that initially, no residual deformation is visible in any of the specimens. With the increase of loading amplitude, the deformation is evident and starts to increase near the bottom of the beam’s web and flange. After the initiation of buckling, the deformation gets higher. By investigating the ultimate failure mode, it is found that all the beams failed by the combination of local and global buckling. Global buckling was comprised both in-plane torsional deformation and out-of-plane flexural deformation. In all beams, local buckling occurred within the bottom region which is around 300 mm above the joint. Moreover, no buckling was noticed in part of the column of all specimens. Figure 3 shows the typical failure mode of the stainless beam-column joint.

To study the cyclic behavior of stainless beam-column joints, the load-displacement and their backbone curves of all FE models are studied. Figure 4 presents the load-displacement curves of some specimens. Well-shaped hysteresis curves are noticed for all specimens. It is observed that with the increase of beam cross-section, the shape of the hysteresis curves is getting steeper, as the bigger section provides more stiffness. For a better understating of cyclic behavior, the backbone curves of all specimens are plotted in Figure 5. As expected, the slope of the elastic part of the backbone curve increases with the increase of the beam cross-section. The yield strength, ultimate strength including corresponding displacement and maximum bending moment of all specimens are listed in Table 2. A similar trend can be noticed in Table 2 that the bigger cross-sections provide higher strength and flexural capacity of the beam in the joint.

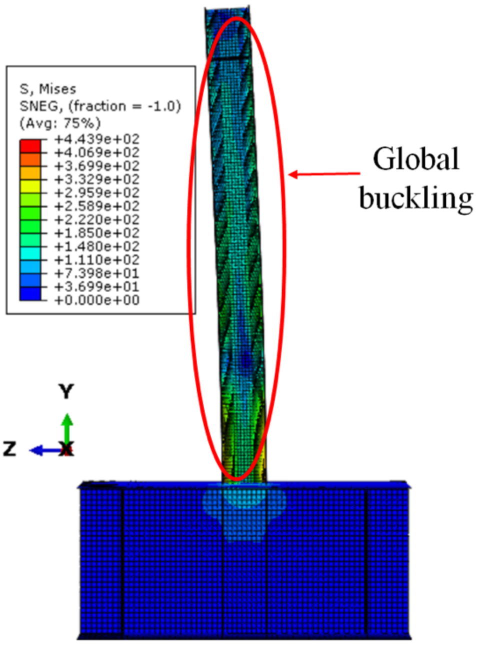

a) Global buckling

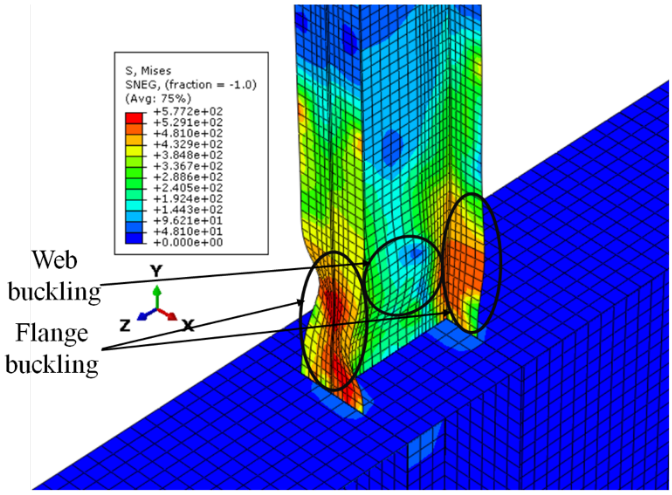

b) Local buckling (flange and web buckling)

Fig. 3: Failure mode of a typical specimen (IPE 180).

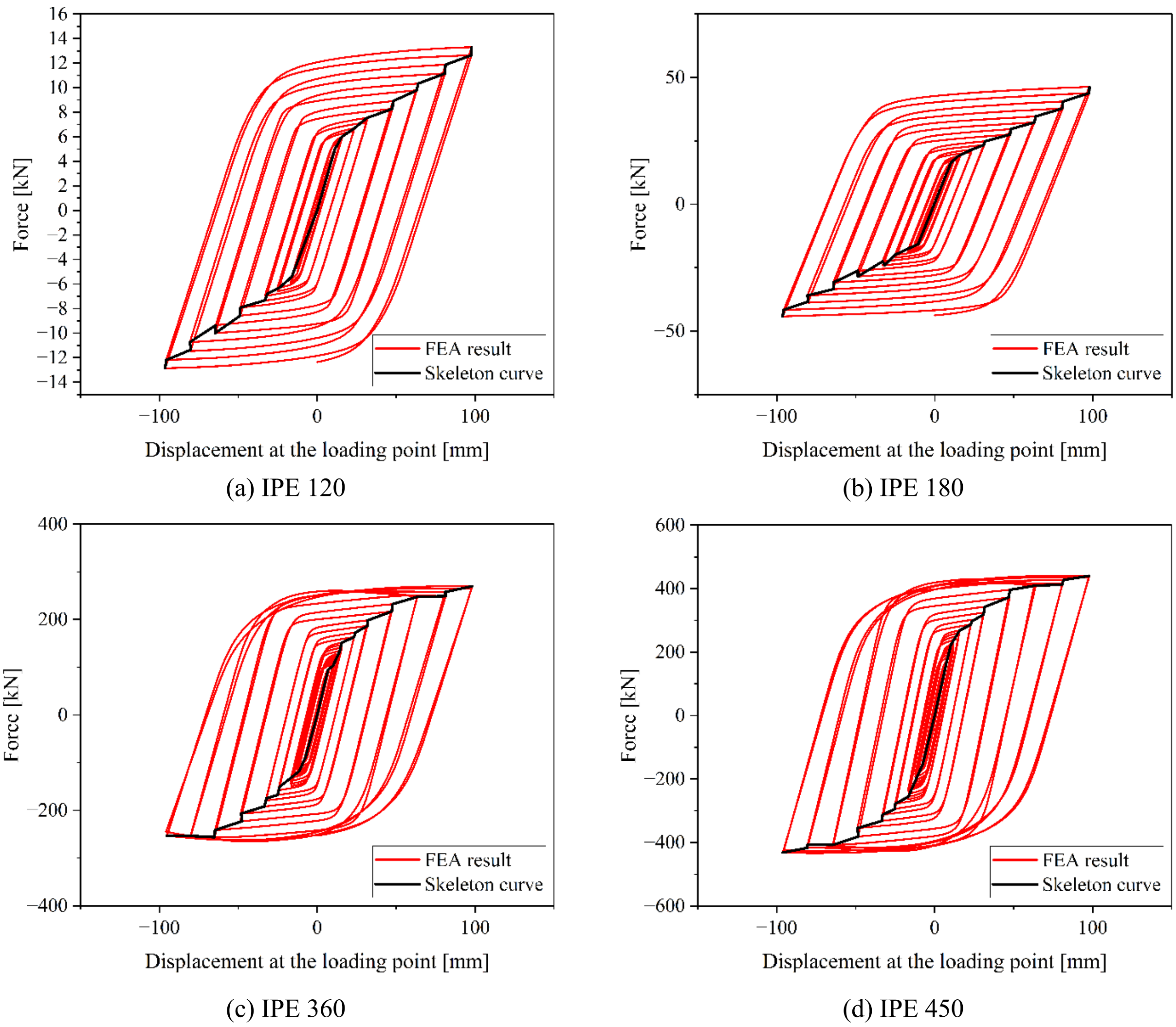

Fig. 4: Load-displacement curves of some specimens.

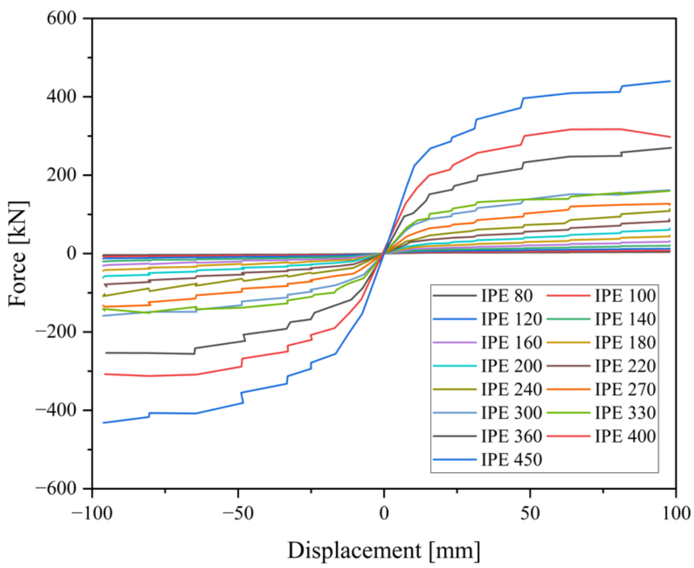

Fig. 5: Backbone curves of all specimens.

Specimen	Yield strength [kN]	Corresponding displacement [mm]	Ultimate strength [kN]	Corresponding displacement [mm]	Maximum bending moment [kN-m]
IPE 80	1.87	15.32	4.23	97.27	6.97
IPE 100	3.58	15.83	7.81	96.84	12.86
IPE 120	5.99	15.54	13.30	97.26	21.91
IPE 140	9.28	15.54	21.22	97.31	34.95
IPE 160	11.57	10.09	32.25	98.01	53.12
IPE 180	16.23	10.13	46.30	97.91	76.26
IPE 200	21.76	11.43	64.18	96.74	105.70
IPE 220	29.30	10.54	87.76	97.69	144.54
IPE 240	36.50	10.85	114.32	96.59	188.29
IPE 270	53.52	11.13	133.91	98.83	220.55
IPE 300	73.34	10.39	162.18	97.01	267.11
IPE 330	84.76	11.34	207.59	98.09	341.91
IPE 360	117.80	11.35	270.14	98.32	444.92
IPE 400	199.97	15.23	329.02	97.93	541.90
IPE 450	224.59	10.37	441.02	97.92	726.36

Table 2: Yield strength, ultimate strength and maximum bending moment of all specimens.

6 CONCLUSIONS

In this study, fifteen FE models of stainless-steel beam-column joint specimens were generated. These models were analyzed under cyclic loading prescribed by AISC to study the cyclic response of these joints. The failure patterns and load-displacement behavior of all specimens were examined. It is observed that the failure pattern of all specimens is the combination of local and global buckling near the bottom region of the beams as columns were considered much stiffer and their movements were restricted than the beams. In local buckling, both web and flange buckling of beam sections were noticed. The load-displacement responses of all specimens show a prominent hysteresis behavior. It is also noticed that the elastic slope of the backbone curve gets steeper for larger cross-sections of the beam as the bigger cross-sections offer more stiffness to the beam. A similar trend was also noticed when comparing the yield strength, ultimate strength and ultimate bending moment of the beam as the larger cross-sections provide higher strength and flexural capacity.

REFERENCES

[1] N.R. Baddoo, Stainless steel in construction: A review of research, applications, challenges and opportunities. *Journal of Constructional Steel Research*, **64**, 1199-1206, 2008.

[2] L. Gardner, Stability and design of stainless steel structures-Review and outlook. *Thin-Walled Structures*, **141**, 208-216, 2019.

[3] K.A. Skalomenos, G.D. Hatzigeorgiou, D.E. Beskos, Parameter identification of three hysteretic models for the simulation of the response of CFT columns to cyclic loading. *Engineering Structures*, **61**, 44–60, 2014.

[4] D.G. Lignos, H. Krawinkler, Development and Utilization of Structural Component Databases for Performance-Based Earthquake Engineering. *Journal of Structural Engineering*, **139**, 1382–1394, 2013.

[5] Eurocode 8 (EC8): *Design of structures for earthquake resistance. 1: General rules, seismic action and rules for buildings*. *EN 1998-1-1.* European Standard (CEN), Brussels, Belgium, 2005.

[6] X. Wei, H. Zhou, G.S. Kamaris, M. Gkantou, F. Yun, X. Zuo, X. Guo, S.B. Ali, Experimental and numerical behaviour of welded stainless steel beam-to-column connections subjected to cyclic loading. *Journal of Constructional Steel Research*, **218**, 108736, 2024.

[7] American Institute of Steel Construction (AISC). *Seismic provisions for structural steel buildings*. AISC, Chicago, 2005.

[8] A.S. Tzimas, G.S. Kamaris, T.L. Karavasilis, C. Galasso, Collapse risk and residual drift performance of steel buildings using post-tensioned MRFs and viscous dampers in near-fault regions. *Bulletin of Earthquake Engineering*, **14**, 1643-1662, 2016.

[9] Abaqus. *Abaqus Documentation*. Dassault Systèmes: Providence, RI, USA. 2022

[10] T. Tafsirojjaman, D.P. Thambiratnam, N.H.R. Sulong, S. Fawzia, Performance of CFRP strengthened full-scale SHS connections subjected to cyclic loading. *Thin-Walled Structures*, **175**, 109211, 2022.

[11] F. Zhou, C. Fang, Y. Chen, Experimental and numerical studies on stainless steel tubular members under axial cyclic loading. *Engineering Structures*, **171**, 72–85, 2018.

[12] K.H. Nip, L. Gardner, A.Y. Elghazouli, Cyclic testing and numerical modelling of carbon steel and stainless steel tubular bracing members. *Engineering Structures*, **32**, 424-441, 2010.

[13] H.X. Yuan, Y.Q. Wang, Y.J. Shi, L. Gardner, Residual stress distributions in welded stainless steel sections. *Thin-Walled Structures*, **79**, 38-51, 2014.